Structure Evolution in Chemical Vapor-Deposited ZnS Films

Everett Y. M. Lee, Nguyen H. Tran, Jennifer J. Russell, and Robert N. Lamb*

Surface Science and Technology Centre, School of Chemical Sciences, University of New South Wales, Sydney NSW 2052, Australia

Received: November 1, 2002

The evolution of the crystallographic structure of ZnS films (thickness ≈ 2 μm) grown on Si(100) wafers by the single-source chemical vapor deposition (CVD) of zinc dimethyldithiocarbamate precursor has been examined. X-ray and electron diffraction indicated that the films were cubic (sphalerite) and oriented preferentially along the (111) direction. Transmission electron microscopy (TEM) indicated that the films were composed of a uniformly distributed array of columns approximately 300−500 nm wide. High-resolution TEM at the interface showed that these columns were attached to the substrate surface via smaller columns (∼50−100 nm wide). The density of crystallographic defects in the bulk columns was lower than that in the interfacial columns. Orientation of the crystallites occurred at a much earlier stage in film growth compared to theoretical predictions for evaporative deposited films, suggesting that the presence of impurities during chemical vapor deposition may influence the structural evolution of the film.

I. Introduction

ZnS is a II−VI semiconductor with a large direct band gap and has many potential applications in areas such as light emission.[1,2] For most thin-film device applications, the film must be highly crystalline and have a particular single crystallographic orientation. Single-source chemical vapor deposition (CVD) is a relatively simple technique that has been used to grow a range of high-quality II−VI semiconductor thin films.[3−11] The technique involves a metal−organic precursor containing the film constituents at the core and attached to a number of organic, volatile ligands. During deposition, the precursor is evaporated onto a heated substrate where it decomposes, leaving behind the film layer while the detached ligands are removed from the deposited system. The single-source CVD technique has also been found to produce conformal films on nonplanar substrates.[12,13]

This paper reports on the growth of zinc sulfide thin films from single-source CVD grown on silicon wafer substrates. Particular emphasis is placed on characterizing the morphology and crystallinity of these films and investigating the various processes occurring at different stages of film growth.

II. Experimental Procedure

The deposition of ZnS films on Si(100) substrates was carried out in a high vacuum chamber with a background pressure of $\sim 2 \times 10^{-7}$ Torr. Zinc dimethyldithiocarbamate $Zn[S_2CNMe_2]_2$ (Pfaltz and Bauer, 99%) was used as the single precursor source. The use of carbamate compounds as precursors in the single-source CVD technique offers the advantage of deposition without the addition of carrier gases.[6−11] During growth, the precursor partial pressure remained at $\sim 2 \times 10^{-5}$ Torr, and the substrate temperature remained at 425 °C. Growth times were varied from ∼4−8 h to produce films approximately 1−2 μm thick.

* Corresponding author. E-mail: r.lamb@unsw.edu.au. Phone: 612 9385 5087. Fax: 612 9662 1697.

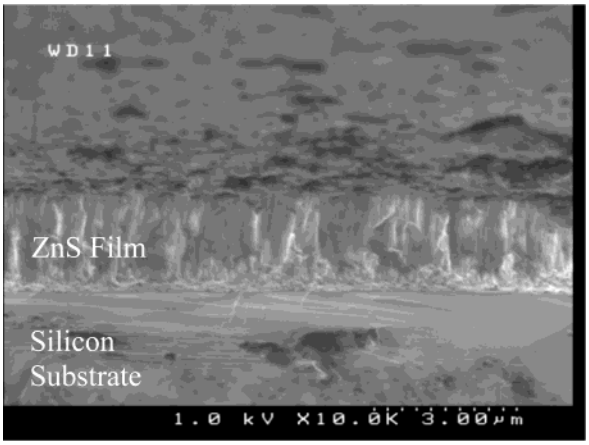

Figure 1. Cross-sectional SEM image of a ZnS film approximately 2 μm thick.

X-ray diffraction was performed using a PW 3040/60 X'Pert Pro diffractometer with an nonmonochromated Cu Kα source ($\lambda = 1.5418$ Å). The microstructure and film morphology were analyzed using a Hitachi 4500 scanning electron microscope. The electron beam was generated with an accelerating voltage of 1 kV. Transmission electron microscopy was performed with a Philips CM200 FEG TEM with an accelerating voltage of 200 kV. Thinning of the samples was performed using an FEI xP200 focused ion-beam miller.

III. Results and Discussion

Figure 1 shows the SEM image of a cleaved edge of a ZnS film grown by single-source CVD of zinc dimethyldithiocarbamate. The film was approximately 2 μm thick and appeared densely packed, without gaps or voids.

Figure 2a and b shows X-ray diffractograms of the single-source CVD ZnS film and a ZnS powder containing both hexagonal and cubic crystallites. The XRD for the ZnS powder was in agreement with the reference.[14] An XRD of a blank silicon (100) wafer is shown in Figure 2c. The peaks at ∼33°

10.1021/jp027366d CCC: $25.00
Published on Web 05/03/2003

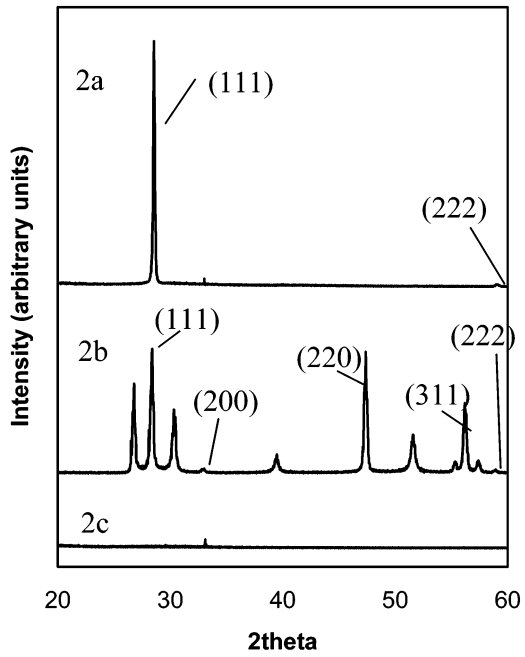

Figure 2. X-ray diffractograms of (a) a ZnS film, (b) ZnS powder containing both hexagonal- and cubic-phase crystallites, and (c) a blank silicon (100) wafer. Note that in the powder spectrum (2b) only the peaks due to reflections from crystal planes in the cubic phase have been labeled.

in Figure 2a and c were both attributed to the Si(200) reflection. The diffraction pattern arising from the film consisted of a single intense peak at ~28.7° due to the fcc (111) reflection and a small peak at ~59° due to the fcc (222) reflection. This indicated that the crystallites in the film have a single preferred (111) orientation.

The TEM image of the cross section of the film is shown in Figure 3a. The bulk of the film consisted of uniformly distributed arrays of columns approximately 300−500 nm in width. These bulk columns did not extend entirely throughout the thickness of the film and were bound to the substrate surface via a uniform array of smaller columns (diameter approximately 50−100 nm). The electron diffractogram of a single large-column crystal from the [101] zone axis is shown in Figure 3b. An origin was assigned away from the central spot to calculate the lattice spacings correctly. After the lattice spacings were calculated, the points were assigned to the diffraction pattern, and it was determined that the ZnS film was cubic. The combined electron and X-ray diffraction results indicated that the films had a preferred orientation along the cubic (111) direction (i.e., the fcc (111) plane was parallel to the substrate). This was expected since the cubic (111) lattice plane has the lowest surface free energy[15] and hence is formed favorably during the deposition of ZnS. The electron diffraction results also indicated that each column had a random orientation within the plane of the substrate. The smearing in the electron diffractogram in Figure 3b was attributed to shearing defects in the (111) plane of the crystallites.

Figure 4 is a typical TEM image of the interfacial area of the film near the surface of the silicon substrate. A key feature is the shape and structure of the small columns that connect the large columns to the substrate. The shearing defects in the (111) plane were also observed in the form of horizontal lines roughly perpendicular to the direction of the columns. These defects, although present throughout the film, were much more abundant in the small columns near the interface. The higher

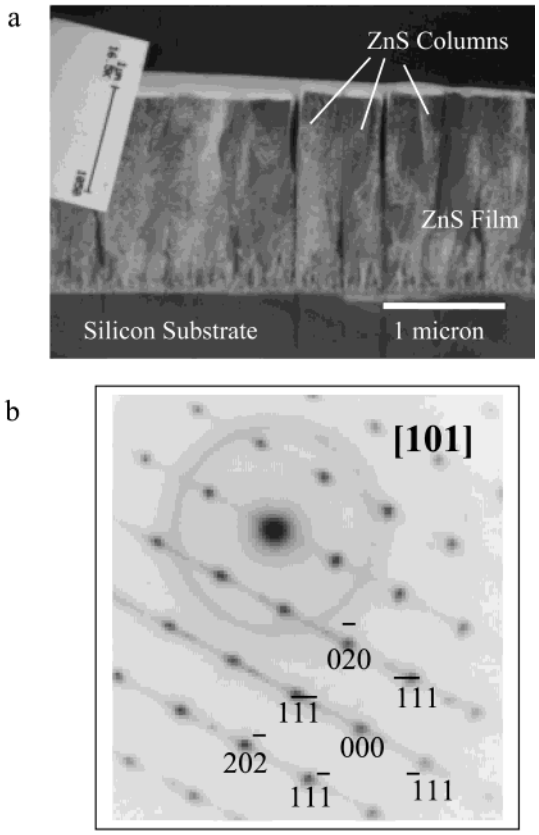

Figure 3. (a) TEM image of the cross section of a ZnS film and (b) an electron diffractogram of a single column within the film.

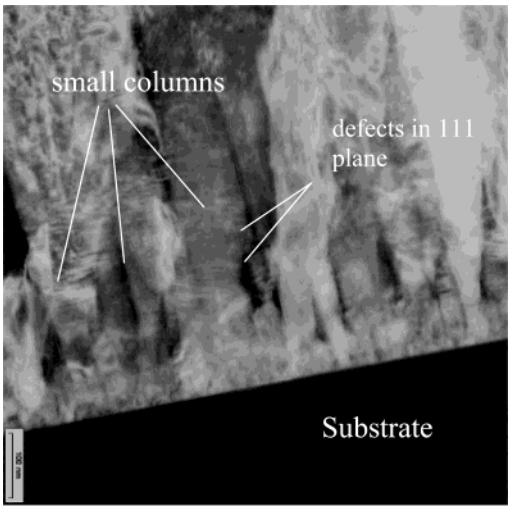

Figure 4. High-magnification image of the small columns near the interface.

concentration of defects in the small columns was attributed to the ordering process that would relieve the lattice mismatch stress, which was much higher at the interface than in the bulk.

The TEM evidence suggests that there are three distinct phases of ZnS film growth. The first stage is nucleation, and although no direct measurements were performed on the initial layers, the presence of columns suggests that island growth occurred (either Volmer−Weber[16] or Stranski−Krastanov[17]). After the initial nucleation stage, small columns were formed that were initially far apart but grew both vertically and laterally until making contact with other columns. Then, through a process of either merging or elimination, the small columns develop into the large columns. The large columns have a fixed

width since they cannot merge with neighboring columns because of differences in plane orientations.

A concise model describing the formation of columnar films in CVD systems has yet to be developed. However, a great deal of literature exists in the form of the structural zone model (SZM) describing the complex processes involved in evaporative film growth. Originally developed by Movchan and Demchishin,[18] the model describes the structural evolution of films as a function of surface mobility and surface free energy. In the original model, three zones were defined by the ratio of substrate temperature (*T*s) to the melting point (*T*m) of the film material. For metal oxides, the ratios were as follows:

$$\frac{Ts}{Tm} < 0.25 \text{ (zone I)}$$

$$0.25 < \frac{Ts}{Tm} < 0.45 \text{ (zone II)}$$

$$0.45 > \frac{Ts}{Tm} \text{ (zone III)}$$

Zone I is dominated by shadowing effects because film crystallites on the surface of the substrate have insufficient energy to reorient into the lowest-energy orientation. The grain boundaries are immobile, leading to the formation of randomly oriented or amorphous films. In zone II, the film crystallites have sufficient energy to reorient themselves into the lowest-energy orientation relative to the substrate. (The grain boundaries are mobile.) As a result of this, zone II films tend to be highly crystalline (with columnar morphology) with a single crystallographic orientation. Thornton[19,20] added a transition zone (zone T) to this model between zones I and II in which some but not all grain boundaries are mobile, leading to the formation of smoother and denser films. By contrast, zone III growth is dominated by bulk diffusion, which leads to the formation of randomly oriented films.

The structural zone models were originally developed through studying thick films (25−300 μm). Adamik and Barna have refined the SZM to include much thinner films ($\sim$1 μm) and have redefined zone T as the "competitive" zone.[21−23] According to Adamik and Barna, zone T growth begins with randomly oriented crystallites. Because of the different growth rates of the crystallographic faces, as the film continues to grow, the fastest-growing orientation begins to dominate and then eventually eliminates the other orientations to produce a columnar morphology with a single orientation. This behavior has been observed or described in a number of studies.[24−28]

From a morphology perspective, the structural evolution of the single-source CVD ZnS film agreed with the modified structural zone model. In particular, the morphology of the small-column region with the expansion and elimination to form large columns was very similar to the morphology of the competitive growth region observed in previous studies.[21−27] However, the XRD detected only reflections due to the fcc (111) plane, suggesting that even at the early stages of film growth (<200 nm) the crystallites within the small columns are not randomly oriented. This was confirmed by additional XRD measurements for relatively thin ZnS films ($\sim$200 nm) that showed only the preferred (111) orientation. These XRD results would initially appear to be contrary to the modified SZM until other orienting factors are considered.

The additional factor behind this contribution is most likely due to the effect of the precursor: in single-source CVD, the deposition of the precursor results in a minute amount of carbon contamination being incorporated into the bulk of the film. Normally, the presence of such an impurity is seen as undesirable but acceptable. It is possible that the SZM for very early stages of film growth (film thickness < 10 nm) is obeyed (i.e., with the formation of randomly oriented crystallites and subsequently with a variety of crystallographic faces exposed). However, carbon contamination that is present would then be most likely to settle preferentially on the crystal faces with the highest surface free energy. Since carbon is a terminating impurity (i.e., the complete coverage of carbon on a ZnS crystal face will inhibit further growth), it is expected that even incomplete coverage will severely restrict the growth of the crystal into which it is incorporated. Given that the (111) plane has the lowest surface free energy, crystallites with this orientation will be the least hindered by carbon contamination. Thus, film growth may begin as randomly oriented crystallites with carbon contamination inhibiting crystallites with a non-(111) orientation. Subsequent growth leads to small columns composed of crystallites with a fcc (111) orientation rather than a random orientation from theoretical predictions and physical deposition.

IV. Conclusions

Single-source CVD with the zinc dimethyldithiocarbamate precursor has been used successfully to produce highly crystalline ZnS films with a cubic (111) orientation. These films were composed of large crystalline columns that were bound to the substrate via smaller columns. The density of defects in these small columns was higher than in the bulk columns. Furthermore, the orientation of the crystallites occurred at a much earlier stage of growth than predicted for evaporative deposited films. These results suggest that the carbonaceous impurities present during precursor decomposition had a significant effect on the evolution of the crystallographic orientation of the film.

Acknowledgment. We thank Paul Munroe for TEM support.

References and Notes

(1) Yamaga, S. *Physica B* **1993**, 185, 500.
(2) Sohn, S. H.; Hamakawa, J. *J. Appl. Phys.* **1992**, *72*, 2492.
(3) Mar, G. L.; Timbrell, P. Y.; Lamb, R. N. *Thin Solid Films* **1993**, *223*, 341.
(4) Mar, G. L.; Timbrell, P. Y.; Lamb, R. N. *Chem. Mater.* **1995**, *7*, 1890.
(5) Tran, N. H.; Lamb, R. N.; Mar, G. L. *Colloids Surf., A* **1999**, *155*, 93.
(6) Tran, N. H.; Hartmann, A. J.; Lamb, R. N. *J. Phys. Chem. B* **2000**, *104*, 1150.
(7) Gleizes, A. N. *Chem. Vap. Depostion* **2000**, *6*, 155.
(8) Pike, R. D.; Cui, H.; Kershaw, R.; Dwight, K.; Wold, A.; Blanton, T. N.; Wernberg, A. A.; Gysling, H. J. *Thin Solid Films* **1993**, *224*, 221.
(9) Nomura, R.; Murai, T.; Toyosaki, T.; Matsuda, H. *Thin Solid Films* **1995**, *271*, 4.
(10) Frigo, D. M.; Khan, O. F. Z.; O'Brien, P. *J. Cryst. Growth* **1989**, *96*, 989.
(11) Afzaal, M.; Aucott, S. M.; Crouch, D.; O'Brien, P.; Woollins, J. D.; Park, J. *Chem. Vap. Deposition* **2002**, *8*, 187.
(12) Lee, E. Y. M. M. Sc. Thesis, University of New South Wales, Sydney, Australia, 2000.
(13) Lee, E. Y. M.; Mar, G. L.; Lamb, R. N. *Proc. SPIE-Int. Soc. Opt. Eng.* **2000**, *4086*, 387.
(14) JCPDS-ICDD file 5-566 for sphalerite.
(15) Wright, K.; Watson, G. W.; Parker, S. C.; Vaughan, D. J. *Am. Mineral.* **1998**, *83*, 141.
(16) Volmer, M.; Weber, A. *Z. Phys. Chem.* **1926**, *119*, 277.
(17) Stranski, I.; Krastanov, L. *Math. Naturwiss. Kl. Iib.*, **1938** *146*, 797.
(18) Movchan, B. A.; Demchishin, A. V. *Fiz. Met. Metalloved.* **1969**, *28(4)*, 653.
(19) Thornton, J. A. *J. Vac. Sci. Technol.* **1974**, *11*, 666.
(20) Thornton, J. A. *Annu. Rev. Mater. Sci.* **1977**, *7*, 239.

(21) Barna, P. B.; Adamik, M. *Thin Solid Films* **1998**, *317*, 27.
(22) Adamik, M.; Barna, P. B.; Tomov, I. *Thin Solid Films* **1998**, *317*, 64.
(23) Adamik, M.; Barna, P. B.; Tomov, I. *Thin Solid Films* **2000**, *359*, 33.
(24) Messier, B.; Yehoda, J. E. *J. Appl. Phys.* **1985**, *58*, 3739.
(25) Yehoda, J. E.; Messier, B. *Appl. Surf. Sci.* **1985**, *22/23*, 590.
(26) Messier, B. *J. Vac. Sci. Technol., A* **1986**, *4*, 490.
(27) Knuyt, G.; Quayhaegens, C.; D'Haen, J.; Stals, L. M. *Thin Solid Films* **1995**, *258*, 159.
(28) Quaeyhaegens, C.; Knuyt, G.; D'Haen, J.; Stals, L. M. *Thin Solid Films* **1995**, *258*, 179.